

AIAA 80-0988R

Study and Experimental Tests of Fibrous Acoustic Treatment for Reduction of Fan Noise from XF3-1 Turbofan Engines

R. Sasaki*

Japan Defense Agency, Tokyo, Japan
and

K. Ishizawa† and K. Higashi‡

Ishikawajima-Harima Heavy Industries Co., Ltd., Tokyo, Japan

The characteristics of an acoustic treatment employing fibrous material and its effect on fan noise reduction radiated from a turbofan engine have been studied. The predominant feature of the treatment is that it is composed of a fibrous layer backed with an air cavity, which facilitates control of the acoustic impedance of the treatment. This paper presents the design procedures for the treatment developed through this study and the results of the tests made to investigate its mechanical and acoustic properties. As a result of acoustic tests using the XF3-1 turbofan engine, it is shown that both discrete and combination tones of the fan can be attenuated effectively by the treatment.

Introduction

ALTHOUGH it is generally recognized that fibrous bulk materials exhibit excellent properties as acoustic treatments, some problems remain to be solved before the materials can be adopted for practical applications. One of these problems is that fibrous materials absorb water, fuel, dirt, etc., which results in deterioration in acoustic effectiveness. It is also of concern to the designers of acoustic treatment whether such materials have enough mechanical strength to withstand the severe environments of aircraft engines.

Recently, however, some fibrous materials have been shown to have the potential for practical applications. A Kevlar felt used in this study is one such material. The mechanical endurance properties of the felt were investigated through such environmental tests as a high-speed air blast, burnthrough, ultraviolet irradiation, and icing. The results of these tests showed that the material has good mechanical properties as an acoustic treatment for actual engines.

Another problem is that acoustic design of such a treatment is usually based on empirical data without the theoretical understanding to relate the acoustic properties to the physical particulars of the material. Therefore, a method to calculate the acoustic properties of the fibrous treatment from its physical properties was considered.

After these preliminary studies, the acoustic treatment to be used in the engine tests was designed. The treatment is composed of a layer of the Kevlar felt with an air cavity behind it. The fan inlet and exhaust treated ducts were designed, fabricated, and acoustically tested using an XF3-1 turbofan engine at an outdoor test facility. Since the engine has a relatively low bypass ratio of 1.9, the engine noise is dominated by jet noise at maximum power in the aft quadrant. Consequently, jet noise was also reduced by mixing the fan and core streams using an internal mixer.

The acoustic data obtained in the tests showed a broad attenuation bandwidth by the acoustic treatment and

significant jet noise reduction effectiveness of the internal mixer.

Engine

The XF3-1 (Fig. 1) is a twin-spool, axial flow turbofan engine with a maximum rated thrust of 1200 kg (2650 lb), a bypass ratio of 1.9, and a fan pressure ratio of 1.67. The engine consists of a single-stage fan and a five-stage compressor driven by single-stage high- and low-pressure turbines, respectively. The fan has 30 blades and 44 stator vanes with a rotor/stator axial spacing of 3 cm (1.2 in.). The fan is 57 cm (22.4 in.) in diameter. The fan tip relative Mach numbers corresponding to the three fan speeds (10,000, 12,000, and 14,700 rpm) at which the acoustic tests were performed are 0.94, 1.11, and 1.34, respectively. The engine has no inlet guide vanes, which augments the fan noise generation.

Noise Reduction Devices

Acoustic Liner

The acoustic treatment used in this research features a fibrous bulk material (Kevlar felt) combined with an air cavity and protected by a perforated aluminum sheet as shown in Fig. 2. The reason for providing the treatment with an air cavity is that the acoustic properties (especially acoustic reactance) can be easily controlled by changing its depth, as will be discussed later.

In order to establish the design procedure for the acoustic treatment mentioned above, the method to predict the acoustic properties from its principal particulars (i.e., the density and thickness of the fibrous material, depth of the air cavity, etc.) was developed at the beginning. This was done using the expressions from Ref. 1 to predict the material's characteristic impedances and propagation constants for the sound propagating in a soft blanket, and considering the boundary conditions in terms of the sound pressure and air particle moving velocity continuation at interfaces between the material and the air. Figure 3 shows the comparison in acoustic properties between the prediction and the data acquired using a standing-wave impedance tube. The prediction method is in reasonable agreement with the measured results if the acoustic liner behaves as a locally reacting one. It is not expected that the liners actually used behave strictly as local reactors, in the sense that the cavity is not divided into Helmholtz-like resonators. However, for simplicity, this method was used to determine the parameters of the acoustic treatment exhibiting the desired impedance.

Presented as Paper 80-0988 at the AIAA 6th Aeroacoustics Conference, Hartford, Conn., June 4-6, 1980; submitted July 23, 1980; revision received March 4, 1981. Copyright © American Institute of Aeronautics and Astronautics, Inc., 1981. All rights reserved.

*Chief Research Engineer, Third Research and Development Center, Technical Research and Development Center.

†Manager, Advanced Applications, Aero-Engine Division.

‡Propulsion Engineer, Advanced Applications, Aero-Engine Division.

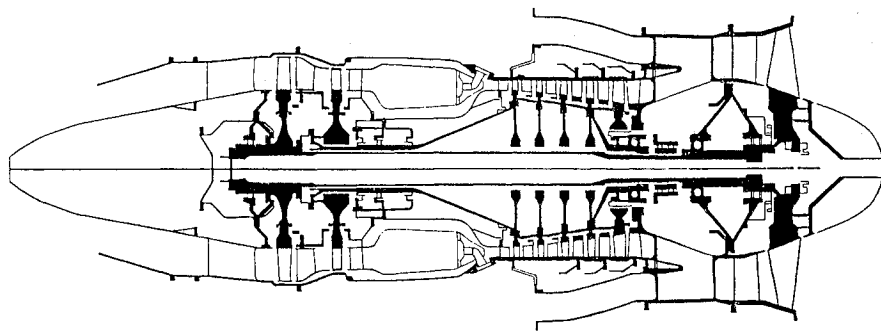


Fig. 1 Schematic section of XF3-1 turbofan engine.

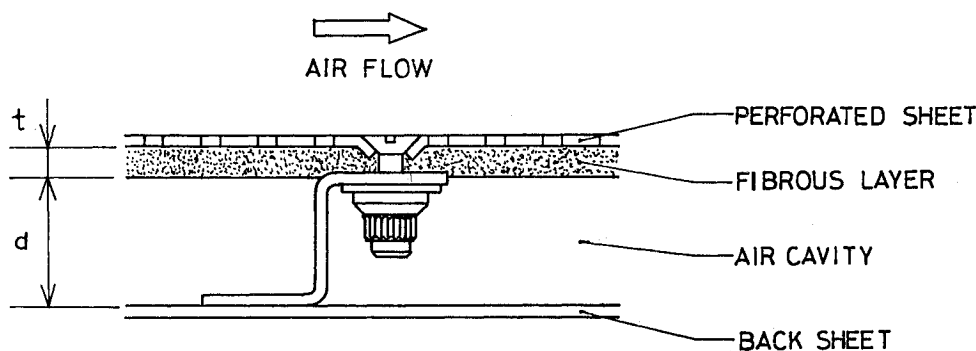
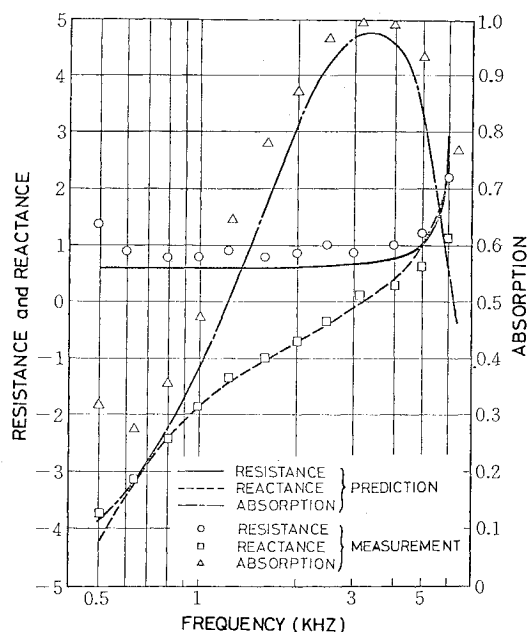


Fig. 2 Structure of acoustic treatment.

Fig. 3 Comparison of predicted acoustic properties of treatment with measurement ($\rho = 0.1 \text{ g/cm}^3$, $t = 5 \text{ mm}$, $d = 20 \text{ mm}$).

On the other hand, the effects of the material density, the air cavity depth, and the material thickness on the acoustic properties were investigated by measuring the acoustic impedances of the treatments over a wide range of these parameters using a standing-wave impedance tube. Figure 4a indicates that varying the material density while keeping the other parameters constant results in a remarkable change in acoustic resistance with only a slight variation in acoustic reactance. Figure 4b shows that varying the air cavity depth results in a variation in acoustic reactance with little variation in acoustic resistance. Figure 4c indicates that varying the material thickness results in major changes in both. From

these results, it is considered that the acoustic resistance and reactance of the treatment with an air cavity can be controlled separately by changing material density and cavity depth, respectively, thus making it easy for the designer to select the parameters of the acoustic treatment that meet the requirements in terms of acoustic properties.

Next, the optimum impedances for the acoustic liners to be applied to the XF3-1 engine were determined using the procedure from Ref. 2. The procedure is based on the analysis of the sound propagation in a circular duct in which, although the effect of the boundary layer is not taken into account, that of the mean flow is. The blade passing frequency at maximum power (7350 Hz) was selected as a design frequency. Figure 5 shows the variation of the optimum impedance with the circumferential mode number m for the propagating conditions at the fan inlet duct. Although the modal energy distribution of the inlet fan noise is not clear, the optimum impedance was determined assuming that the energy was concentrated in the mode whose circumferential lobe number is equal to the number of fan blades—something likely to occur in the case of forward radiated noise from the fan without inlet guide vanes ingesting an undistorted flow. Thus, the optimum impedance selected for the fan inlet liner was $2.6\text{--}0.63 i$. The optimum impedance for the fan exhaust liner was determined in a similar way. In this case, however, the least attenuated mode was assumed to be dominant, based on the results of the authors' earlier study.² The optimum impedance selected for the fan exhaust liner was $0.78\text{--}0.39 i$.

Then, the leading particulars of the acoustic treatments to have the properties mentioned above were determined using the method stated earlier. The results are shown in Table 1. The acoustic properties of these treatments were demonstrated by impedance tube tests to satisfy the acoustic requirements.

Acoustic liners were fabricated using the Kevlar felt treatment with epoxy resin and covered with a perforated sheet with an open area ratio of 30%, which is large enough to avoid effects on the acoustic properties of the material. The length of the fan inlet liner was 45 cm (17.7 in.) and the ratio

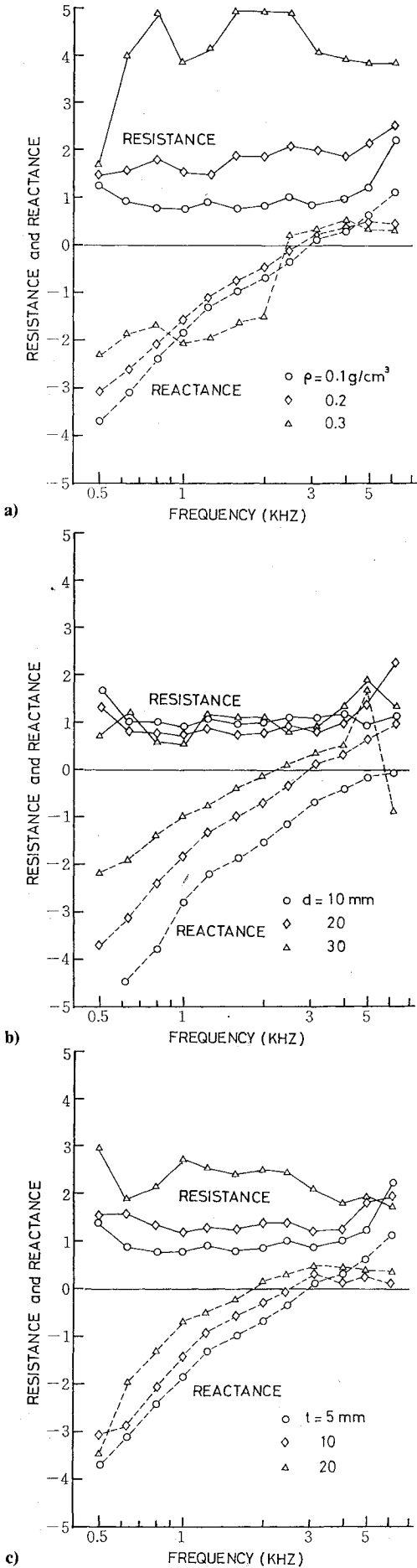


Fig. 4 Effect of leading parameters of treatment on acoustic impedance. a) Density variation ($t = 5$ mm, $d = 20$ mm). b) Cavity depth variation ($\rho = 0.1$ g/cm³, $t = 5$ mm). c) Felt thickness variation ($\rho = 0.1$ g/cm³, $d = 20$ mm).

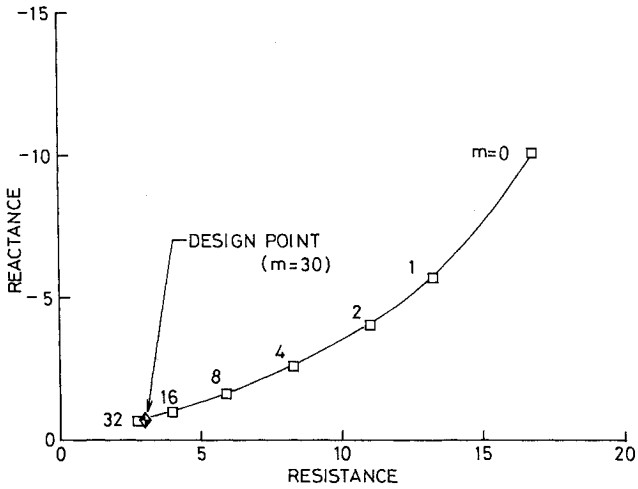


Fig. 5 Optimum impedance for the XF3-1 inlet treatment at maximum speed (BPF = 7350 Hz, inlet flow Mach number = 0.4, inlet diameter = 0.6 m).

Table 1 Leading parameters of the acoustic treatment

Parameters	Fan inlet treatment	Fan exhaust treatment
Felt thickness	3 mm (0.118 in.)	2 mm (0.079 in.)
Cavity depth	10 mm (0.394 in.)	12 mm (0.472 in.)
Felt density	0.2 g/cm ³ (11.9 lb/ft ³)	0.2 g/cm ³ (11.9 lb/ft ³)

of length to duct diameter was 0.75, and the length of the fan exhaust liner was 25 cm (9.8 in.) and the ratio of length to duct height was 4.2.

Internal Exhaust Mixer

Since the XF3-1 engine has a relatively low bypass ratio of 1.9, its noise is characterized by jet noise at maximum power in the aft quadrant. Therefore, jet noise should also be attenuated to achieve sufficient reduction in the total engine noise.

In order to determine the best way to attenuate the jet noise of the XF3-1, several kinds of exhaust mixers were tested from aerodynamic and acoustic points of view using one-fifth scale models under simulated exhaust conditions. As a result, the internal mixer was selected because its large noise attenuation resulted in the least loss of aerodynamic performance. It was also preferable because its installation required the least modification and therefore the lowest weight increase in the engine.

The internal mixer for the full-scale engine tests was designed using the experimental data obtained through the scale-model tests mentioned above. The mixing nozzle (located in the outer duct and used to mix the bypass and core streams) has 12 lobes. This number of lobes was determined from a manufacturing point of view, although it has been shown that the greater the number of lobes, the higher the noise attenuation. (Needless to say, the pressure loss also increases as the number of lobes increases.) The areas at the mixing plane of the two streams were determined so that the static pressure of the streams at the discharge would be equal in order to eliminate undesirable effects on engine operation resulting from a mismatch of high- and low-pressure systems. Mixer shapes were determined so as to eliminate local flow separation due to the excessive flow turning and diffusion rate.

Acoustic Tests

Test Facility and Instrumentation

The acoustic tests were conducted to investigate the characteristics of the XF3-1 engine noise and the effectiveness

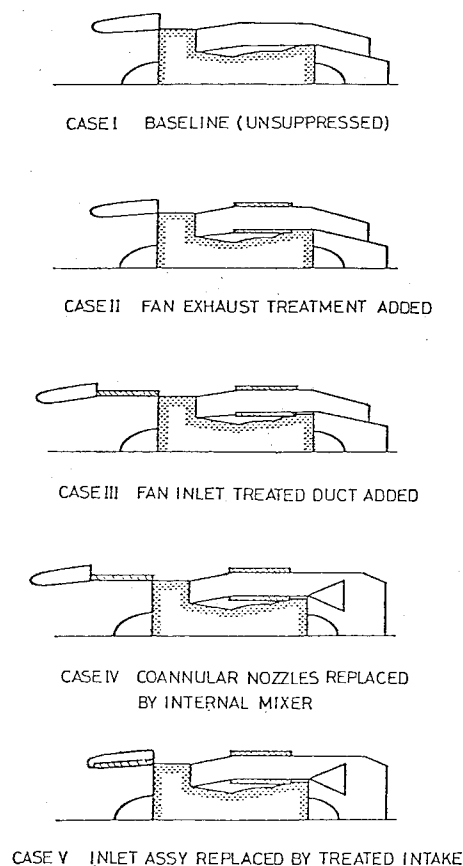


Fig. 6 Acoustic test configurations.

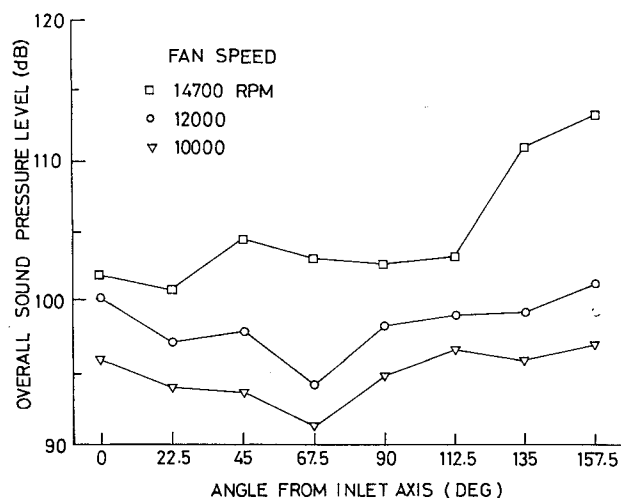


Fig. 7 Directivity of XF3-1 engine noise in the baseline configuration (case I) measured on a 30 m radius.

of the noise reduction devices at an outdoor test facility. The test area is paved with concrete in the vicinity of the engine stand and the other portion of the area is covered by a dead grass.

The XF3-1 engine was hung up to a test stand 1.8 m (6 ft) above the ground. The engine was controlled and monitored at a control room located 15 m (50 ft) from the engine.

Eight 12.7 mm ($\frac{1}{2}$ in.) condenser microphones were positioned 1.2 m (4 ft) above the ground at 22.5 deg intervals from 0 to 157.5 deg (measured from the engine inlet axis) on a 30 m (150 ft) radius.

The microphone signals were transmitted to the noise measuring room through shielded cables and amplified for frequency modulation recording on an Ampex 1300A data

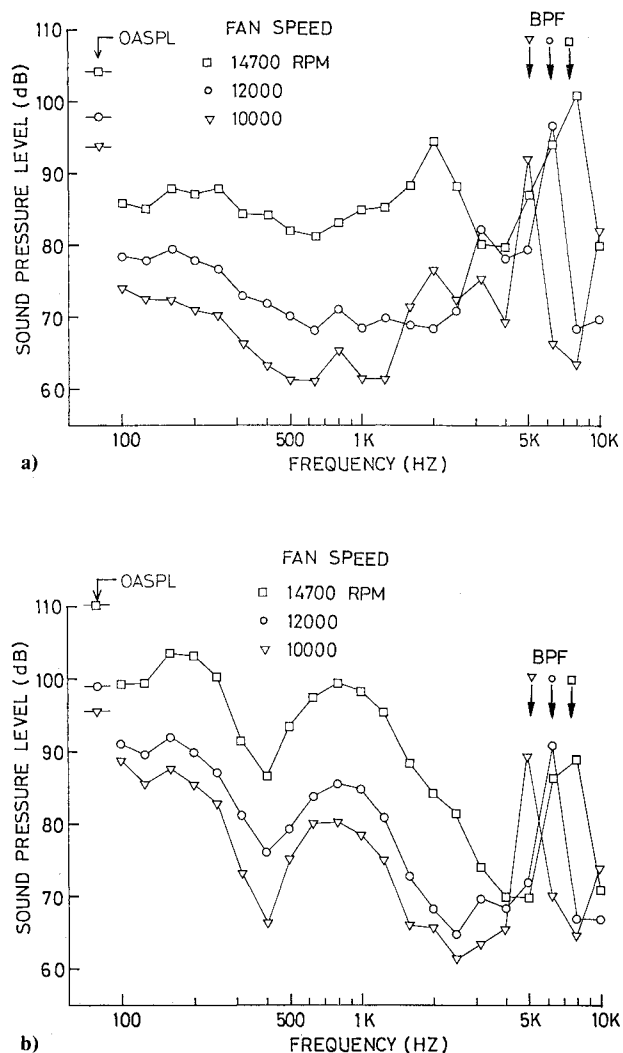


Fig. 8 Baseline engine noise spectra. a) Forward quadrant (at 45 deg on a 30 m radius). b) Aft quadrant (at 135 deg on a 30 m radius).

recorder. The acoustic system was calibrated using a 124 dB reference signal generated by a pistone phone before each engine run.

Test Procedure

Five configurations shown in Fig. 6 were tested in this investigation. The baseline (case I) is the unsuppressed configuration and consists of a flight-type intake resembling the inlet section of an actual nacelle, hard wall fan exhaust ducts, and coannular exhaust nozzles. Other configurations were developed by replacing these devices with others adopting noise reduction concepts. Through these tests, the noise attenuating effectiveness of the fan inlet and exhaust acoustic liners and the internal mixer was investigated by comparing one configuration to the other.

The engine was run at three fan mechanical speeds, i.e., 10,000 (68%), 12,000 (82%), and 14,700 (100%) rpm; thrusts at these speeds in the baseline configuration were 350 kg (772 lb), 680 kg (1500 lb), and 1160 kg (2560 lb), respectively. Noise measurement was carried out in ascending order of fan speed and this measurement series was repeated twice in each configuration.

Results and Discussion

One-third octave band analyses were performed by playing back the magnetic tapes containing the microphone signals obtained during the acoustic tests. On the basis of these

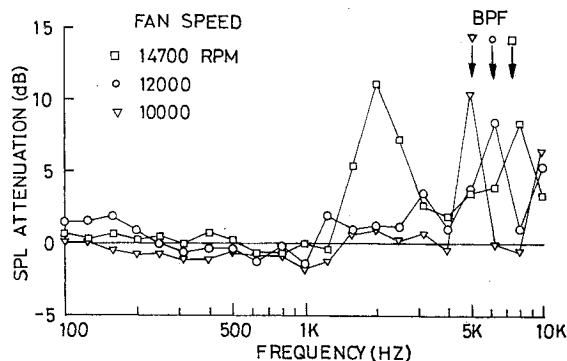


Fig. 9 Sound pressure attenuation spectra of the treatment on additional inlet duct at 45 deg.

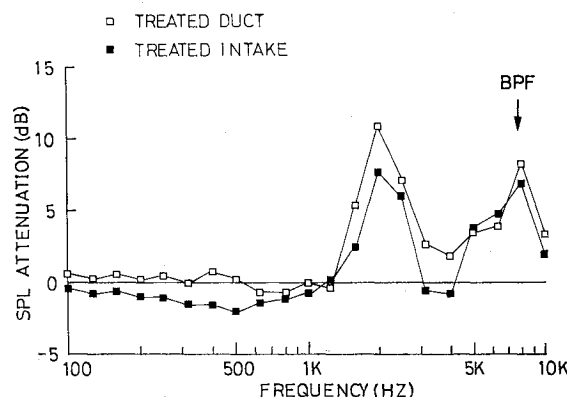


Fig. 10 Comparison of attenuation spectra of the treatments on additional inlet duct and integrated to the intake at 45 deg and maximum power.

analyses, the characteristics of the baseline unsuppressed engine noise, the effects of the noise reduction devices on them, etc., are discussed below.

Baseline Engine Noise

Figure 7 shows the directivities of the overall sound pressure level (OASPL) of the XF3-1 engine in the baseline configuration (case I) at the three fan rotor speeds. Although the noise levels in the forward and aft quadrants are almost the same at low- and medium-power settings (10,000 and 12,000 rpm), the aft-quadrant noise becomes dominant at maximum power (14,700 rpm).

To investigate the characteristics of the noise in both quadrants more closely, the one-third octave band spectra at the 45 and 135 deg positions are shown in Figs. 8a and 8b, respectively. At 45 deg, it is indicated that the noise is dominated by the fan blade passing frequency (BPF) tone and its harmonic from low to maximum power with significant contribution of the multiple pure tones (MPT) around 2 kHz at maximum power.

On the other hand, at 135 deg the BPF tone is remarkable only at low and medium power and the dominance in the aft-quadrant noise is taken over by the overwhelming jet noise at maximum power. The significant increase in the aft-quadrant OASPL at maximum power is due mainly to the contribution of jet noise.

Effectiveness of Fan Inlet Treatment

As was shown by the schematics in Fig. 6, the fan inlet acoustic liner was tested in two forms. One was on a separate duct as in cases III and IV and the other was integrated onto the flight-type intake as in case V. In the former cases, the total length of the inlet assembly including the hard wall portion was twice that of the latter case, although the liner lengths were the same in both cases.

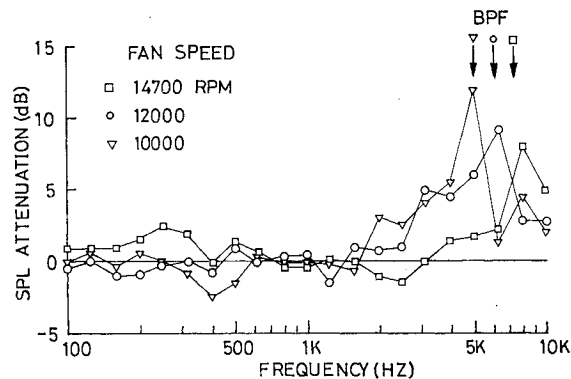


Fig. 11 Sound pressure attenuation spectra of fan exhaust treatment at 135 deg.

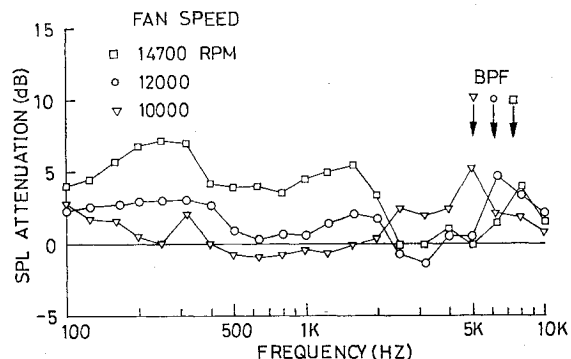


Fig. 12 Sound pressure attenuation spectra of exhaust inlet mixer.

The effect of the treated extra duct is shown by the attenuation spectra at 45 deg in Fig. 9 (obtained from the comparison of cases III and II). There are attenuation peaks at the BPF and its harmonic at all fan speeds is shown and, in addition, another peak is observed at the frequency region corresponding to the MPTs (in the vicinity of 2 kHz) at maximum power.

The treatment has higher BPF attenuation at 10,000 rpm than at the other two speeds in spite of the selection of the design frequency at the maximum power BPF. This is probably because the BPF tone of 10,000 rpm consists of a mode with a lower cutoff ratio than at higher power, thus having higher maximum possible attenuation.

Of more interest from a practical point of view is the performance of the treatment integrated to the flight-type intake. Figure 10 shows a comparison of the attenuation spectra of the treated separate duct and the treated flight-type intake at maximum power. (The latter attenuation spectrum was obtained by comparing cases V and II.) The integrated fan inlet treatment exhibits almost the same attenuation against the BPF and slightly less attenuation against the MPTs compared with the treated separate duct.

Effectiveness of Fan Exhaust Treatment

The effect of the fan exhaust treatment on the engine noise is shown in Fig. 11 by the attenuation spectra for the three fan speeds (the result of comparison of cases II and I). All of the attenuation spectra have peaks at BPF as do those of the fan inlet treatment. However, because the MPTs are not as significant in the aft quadrant as in the forward quadrant, no obvious peak can be observed at MPT frequencies.

The peak attenuation at the BPF is highest at 10,000 rpm and decreases with the increase of engine power in spite of the treatment design frequency selected at the BPF corresponding to maximum fan speed. This may be because that the BPF tone at the lower fan speed is of the lower frequency parameter, or the ratio of duct width to wavelength, and thus has the higher maximum possible attenuation.

Effectiveness of Internal Mixer

The noise reduction effectiveness of the internal mixer is shown in Fig. 12 by the attenuation spectra for the three fan speeds at 135 deg (the result of comparing cases IV and III). At low power, where the jet noise is not so dominant, the effectiveness of the mixer is not apparent except that a small peak can be observed at the BPF. With the increase of the engine power, the attenuation at the low-frequency portion corresponding to the jet noise becomes more apparent. At maximum rating, the attenuation was observed over a wide range of 0.1 to 2.5 kHz with the highest 7.5 dB at 250 Hz.

In addition to the jet noise reduction, the attenuation at the BPFs is also noted at all speeds. This may result from the shielding effect on the fan BPF tone caused by the outer case of the internal mixer.

On the other hand, the comparison of performance data of the configurations with and without the internal mixer indicated the thrust loss of 4.1% in the configuration with the mixer at the same fan speed near maximum. This thrust loss, however, is due mainly to the decrease in total engine airflow of 3.7%; the increase in specific fuel consumption is only 0.6%. This means that the exhaust nozzle area is a little too small and a large portion of the loss is expected to be recovered by closer adjustment of the area.

Conclusions

The acoustic treatment consisting of a fibrous material and an air cavity has been designed, fabricated, and tested using an XF3-1 turbofan engine. In the acoustic tests, the noise attenuation effectiveness of the internal mixer to reduce jet noise which dominates the engine noise in the aft quadrant at a high power setting has also been investigated.

The test results showed that the treatment has such a broad attenuation bandwidth that the fan rotating noise extending over wide frequencies (i.e., the BPF tones and their harmonics from low to maximum power settings, and the multiple pure tones generated at a high power setting) can be attenuated effectively. It was also shown that the introduction of an internal mixer to the XF3-1 turbofan engine results in a significant reduction of the jet noise.

References

- ¹Beranek, L. L., *Noise Reduction*, McGraw-Hill Book Co., New York, 1960, pp. 247-279.
- ²Sasaki, R. and Ishizawa, K., "Study on Fan Noise Characteristics and Fan Noise Abatement Technology," *Journal of the Japan Society for Aeronautical and Space Sciences*, Vol. 27, 1979, pp. 585-594.

From the AIAA Progress in Astronautics and Aeronautics Series . . .

AEROACOUSTICS: FAN, STOL, AND BOUNDARY LAYER NOISE; SONIC BOOM; AEROACOUSTIC INSTRUMENTATION—v. 38

Edited by Henry T. Nagamatsu, General Electric Research and Development Center; Jack V. O'Keefe, The Boeing Company; and Ira R. Schwartz, NASA Ames Development Center

A companion to Aeroacoustics: Jet and Combustion Noise; Duct Acoustics, volume 37 in the series.

Twenty-nine papers, with summaries of panel discussions, comprise this volume, covering fan noise, STOL and rotor noise, acoustics of boundary layers and structural response, broadband noise generation, airfoil-wake interactions, blade spacing, supersonic fans, and inlet geometry. Studies of STOL and rotor noise cover mechanisms and prediction, suppression, spectral trends, and an engine-over-the-wing concept. Structural phenomena include panel response, high-temperature fatigue, and reentry vehicle loads, and boundary layer studies examine attached and separated turbulent pressure fluctuations, supersonic and hypersonic.

Sonic boom studies examine high-altitude overpressure, space shuttle boom, a low-boom supersonic transport, shock wave distortion, nonlinear acoustics, and far-field effects. Instrumentation includes directional microphone, jet flow source location, various sensors, shear flow measurement, laser velocimeters, and comparisons of wind tunnel and flight test data.

509 pp. 6 x 9, illus. \$19.00 Mem. \$30.00 List

TO ORDER WRITE: Publications Dept., AIAA, 1290 Avenue of the Americas, New York, N. Y. 10019